Published in final edited form as:

J Environ Pathol Toxicol Oncol. 2018 ; 37(4): 317–329. doi:10.1615/JEnvironPatholToxicolOncol.2018028689.

Investigating the Role of Mitochondrial Respiratory Dysfunction during Hexavalent Chromium-Induced Lung Carcinogenesis

James T.F. Wise[a], **Lei Wang**[b], **Michael C. Alstott**[c], **Ntube N.O. Ngalame**[b], **Yuting Wang**[b], **Zhuo Zhang**[d], and **Xianglin Shi**[a,b,d,*]

[a]Division of Nutritional Sciences, Pharmacology and Nutritional Sciences, College of Medicine, University of Kentucky, Lexington, KY

[b]Center for Research on Environmental Disease, College of Medicine, University of Kentucky, Lexington, KY

[c]Markey Cancer Center, Redox Metabolism Shared Resource Facility, University of Kentucky, Lexington, KY

[d]Toxicology and Cancer Biology, College of Medicine, University of Kentucky, Lexington, KY

Abstract

Hexavalent chromium [Cr(VI)] is a lung carcinogen and its complete mechanism of action remains to be investigated. Metabolic reprogramming of key energy metabolism pathways (e.g., increased anaerobic glycolysis in the presence of oxygen or “Warburg effect,” dysregulated mitochondrial function, and lipogenesis) are important to cancer cell and tumor survival and growth. In our current understanding of Cr(VI)-induced carcinogenesis, the role for metabolic reprogramming remains unclear. In this study, we treated human lung epithelial cells (BEAS-2B) with Cr(VI) for 6 months and obtained malignantly transformed cells from an isolated colony grown in soft agar. We also used Cr(VI)-transformed cells from two other human lung cell lines (BEP2D and WTHBF-6 cells). Overall, we found that all the Cr(VI)-transformed cells had no changes in their mitochondrial respiratory functions (measured by the Seahorse Analyzer) compared with passaged-matched control cells. Using a xenograft tumor growth model, we generated tumors from these transformed cells in Nude mice. Using cells obtained from the xenograft tumor tissues, we observed that these cells had decreased maximal mitochondrial respiration, spare respiratory capacity, and coupling efficiency. These results provide evidence that, although mitochondrial dysfunction does not occur during Cr(VI)-induced transformation of lung cells, it does occur during tumor development.

Keywords

chromium; mitochondria; Seahorse Analyzer; metabolism; lung; hexavalent chromium

*Address correspondence to: Xianglin Shi, PhD, Center for Research on Environmental Disease, 1095 V.A. Drive, 306 Health Sciences Research Building, Lexington, KY 40536; Tel.: 859-257-4054; Fax: 859-323-1059, xshi5@uky.edu.

I. INTRODUCTION

Hexavalent chromium [Cr(VI)] is a known human lung, nasal, and esophageal carcinogen.[1–5] Epidemiological studies of Cr(VI)-exposed workers have reported up to an 80-fold increased risk of developing lung cancers.[4] Although the exact mechanism of chromate-induced lung cancer remains elusive, there are multiple mechanisms reported in the literature: (1) Cr(VI) is a potent genotoxic agent that acts as a carcinogen by inducing DNA double-strand breaks, chromosome instability, altered DNA repair, and other genomic alterations[6–8]; (2) Cr(VI) generates reactive oxygen species that cause downstream alterations in protein signaling and redox metabolism imbalance[1–5]; (3) Cr(VI) is able to increase epidermal growth factor receptor (EGFR) expression; and (4) Cr(VI) is able to induce angiogenesis.[1–3] Some evidence suggests that Cr(VI) is able to induce altered cellular energetics.[9–11] Cr(VI) is also able to directly activate upstream factors that regulate metabolism in human cells or alter metabolic pathway signaling patterns.[12] We propose that Cr(VI)-altered energy metabolism occurs in the mechanism of Cr(VI)-induced carcinogenesis.

Altered cellular metabolism was first proposed to be an underlying feature of cancer cells as early as the 1920s.[13–15] There is growing evidence that cancer cells have increased glycolysis with an increase in lactic acid fermentation of pyruvate (or anaerobic glycolysis), where normal cells have a lower levels of glycolysis and low levels of lactic acid fermentation with a high oxidation of pyruvate in mitochondria (or aerobic glycolysis). This change in the usage of pyruvate after glycolysis persists even in the presence of physiological or ambient oxygen levels, appears to be a permanent shift to anaerobic glycolysis, and has subsequently been termed the “Warburg effect”.[16,17] This altered energy usage is important for the survival of cancer cells and may provide these cancer cells survival advantages in the tumor microenvironment.[16,17] Other energy metabolism pathways have been shown to be altered in cancer cells, such as high rates of energy-consuming processes of DNA synthesis and protein synthesis. Similarly, increased lipogenesis in cancer cells is found to be vital to cancer cell survival and growth.[16–18] Mitochondrial dysfunctions and alterations to mitochondrial respiration have been associated with cancer and tumor progression.[19] All of the aforementioned alterations of cellular energetics have recently been considered hallmarks of cancer.[16–18]

Given the vast reporting on the importance of metabolic changes in cancer, there remains sparse literature on the role of mitochondrial dysfunction during the carcinogenesis processes. Due to recent advancements in our understanding of cellular energetics and the development of tools to functionally measure metabolism (i.e., the Seahorse Analyzer), we can now directly analyze mitochondrial respiration. There are some literature reports investigating mitochondrial respiration during transformation of human cell lines; for example, one study reported that mitochondrial dysfunction plays an important role in pancreatic carcinogenesis, whereas another found that mitochondrial dysfunction is important in prostate carcinogenesis.[20,21]

When examining mitochondrial changes, there are multiple end points: mitochondrial DNA, mitochondrial membrane potential, mitochondrial structure, mitochondrial respiratory

functions, and the different complexes in the mitochondria. To investigate mitochondrial changes in Cr(VI) carcinogenesis, we chose to study the role of mitochondrial respiratory dysfunction. We exposed human bronchial epithelial airway cells (BEAS-2B) to low concentrations of sodium chromate for 6 months and then isolated an individual colony from soft agar and characterized the metabolism of these cells. We compared our malignantly transformed cells against two sets of Cr(VI)-transformed lung cell lines and passage-matched control cells from previous chromium studies, which originated from immortalized human lung bronchial cells (BEP2D cells) and immortalized human lung fibroblasts (WTHBF-6 cells).[8,22] We carried out tumorigenesis studies by employing a xenograft tumor growth model using Nude mice and subcutaneously grafting each of the Cr(VI)-transformed lung cells. Then, we isolated xenograft-tumor derived cells from xenograft tumor tissues. These xenograft-tumor derived cells closely mimic cell lines derived from a tumor.

Our data showed no major mitochondrial respiration changes were observed in Cr(VI)-transformed cells compared with their passaged-matched control cells. However, we observed that xenograft tumor-derived cells had decreased maximal mitochondrial respiration and spare respiratory capacity (or respiratory reserve) of the mitochondria compared with Cr(VI)-transformed cells and passaged-matched control cells. These results indicate that there is no change in mitochondrial respiration during Cr(VI)-induced transformation, but mitochondrial respiration is decreased during tumor development, possibly due to the tumor microenvironment.

II. MATERIALS AND METHODS

A. Reagents

Sodium chromate, glutamine (for Seahorse tests), oligomycin, 2-deoxyglucose, rotenone, and antimycin A were from Sigma-Aldrich (St. Louis, MO, USA). Trypsin/EDTA, sodium pyruvate, penicillin/streptomycin, LHC media, and L-glutamine were from Thermo Fisher Scientific (Waltham, MA, USA). Dulbecco's minimal essential medium and Ham's F-12 medium (DMEM/F-12) were from Mediatech (Herndon, VA, USA). Cosmic calf serum was from Hyclone (Logan, UT, USA). Collagenase Type II was from STEMCELL Technologies (Vancouver, Canada) Tissue culture dishes, flasks, and plastic ware were from Falcon Labware (Becton-Dickinson, Franklin Lakes, NJ, USA). Carbonyl cyanide-p-trifluoromethoxyphenylhydrazone (FCCP) and XF base medium were from Agilent Technologies (Santa Clara, CA, USA).

B. Cell Culture

BEAS-2B, BEP2D, and WTHBF-6 were used as model human lung cells. BEAS-2B are SV40 immortalized human bronchial airway cells that were obtained from ATCC.[23] BEP2D cells are HPV-immortalized human bronchial epithelial cells that were received as a gift from Dr. Curtis Harris at the National Institutes of Health (NIH).[24] WTHBF-6 cells are hTERT-expressing human lung fibroblasts that were received as a gift from Dr. John P. Wise, Sr. at the University of Louisville.[25] WTHBF-6 and Cr(VI)-transformed WTHBF-6 cell lines were cultured in a 50:50 mixture of Dulbecco's minimal essential medium and Ham's F12 medium plus 15% cosmic calf serum, 1% L-glutamine, and 1% penicillin/streptomycin.

BEAS-2B and Cr(VI)-transformed BEAS-2B cell lines were cultured in LHC-9 medium. BEP2D and Cr(VI)-transformed BEP2D cell lines were cultured in LHC-8 medium. All cells were maintained in a 37°C, humidified incubator with 5% CO_2. At least once a week, cells were subcultured using 0.25% trypsin/1 mM EDTA solution and all experiments were performed on logarithmically growing cells.

C. Preparation of Chromium Compounds

Sodium chromate (Na_2CrO_4) is a soluble form of Cr(VI) and was administered as a solution in water as described previously.[26]

D. Chromium Time Course

BEAS-2B cells were exposed to sodium chromate (0.5 μM) for 6 months (180 days) and routinely cultured with sodium chromate re-added during subculturing and when the medium was refreshed (48–72 hours). Passage-matched control BEAS-2B cells were cultured alongside the two treatment groups. Following 6 months of exposure, cells were seeded into agar and an individual colony from the 0.5 μM treatment group was isolated. Passaged-matched control BEAS-2B cells were cultured alongside the agar dishes.

E. Seahorse Extracellular Flux Analysis

The Seahorse XF96 Extracellular Flux Analyzer (Agilent Technologies) was used to measure mitochondrial respiration activity in all cells. Twenty-four hours prior to the assays BEAS-2B, BEP2D, and WTHBF-6 cells were seeded at a density of 4.0×10^4, 4.5×10^4, and 3.5×10^4 cells per well in a XF96 plate, respectively. The seeding densities used for the Cr(VI)-transformed cells were the same as their passaged-matched control cells. The mitochondrial stress tests were performed per manufacturer's protocol. For the basal medium for the experiments, we used XF base medium with 25 mM glucose, 2.0 mM glutamine, and 1.0 mM pyruvate. During the assay, the values used for injections were 100 μM oligomycin and 50 mM 2-deoxyglucose. For the injections of FCCP BEAS-2B, control and transformed cell lines received 0.3 μM FCCP and BEP2D and WTHBF-6 control and transformed cell lines received 0.6 μM FCCP. Data were normalized to baseline read for the third oxygen consumption read and are presented as a percentage.[27] Coupling efficiency was not normalized as to the baseline third oxygen read given that it has an internal normalization in its calculation. The basal respiration, maximal respiration, spare respiratory capacity, coupled respiration, coupling efficiency, non-mitochondrial oxygen consumption, and proton leak were calculated using the Seahorse Wave software for XF analyzers. All Seahorse experiments were performed in at least triplicate by the Redox Metabolism Shared Resource Facility at the University of Kentucky.

F. Soft Agar Assay and Colony Isolation

To confirm malignant transformation of the Cr(VI) treated BEAS-2B cells had occurred, an anchor-age-independent cell growth assay was used. Soft agar colony formation assays were performed as described previously.[28] Briefly, 2 mL of 0.67% agar in LHC-9 medium was placed into each well of a six-well culture plate. A suspension (2 mL) containing 5×10^4 cells was mixed with 2 mL of 0.33% agar-LHC-9 and placed on the previous bottom layer of

the agar and grown for 8 weeks. Twenty-four hours after plating, cultures were examined microscopically to confirm an absence of large clumps of cells. Colonies were stained with 5% 4-Nitroblue tetrazolium chloride. To establish cultures from anchor-age-independent colonies, one soft-agar colony was plucked under sterile conditions and then dispersed in trypsin and re-plated into culture dishes.

G. Xenograft Studies

The animal studies were conducted in accordance with NIH animal use guidelines and the experimental protocol approved by the institutional animal care and use committee of the University of Kentucky at Lexington. Athymic Nude mice (NU/NU, 6–8 weeks old; The Jackson Laboratory) were housed in a pathogen-free room in the animal facilities at the Chandler Medical Center, University of Kentucky. Cells (1×10^6 cells per mouse) from each cell line were re-suspended in serum-free medium with basement membrane matrix (BD Biosciences) at a 1:1 ratio (total volume = 100 μL) and subcutaneously injected into the flanks of Nude mice for up to 6 months. There were a total of eight injection sites per cell line used; each mouse received one subcutaneous injection per side (a total of eight mice were used per experiment). Mice were checked daily for tumor appearance. At the end of the experiment, mice were sacrificed and tumors were excised into pieces to be snap frozen or to be used for cell line development. Tumor volume was determined by Vernier caliper, following the formula of $A \times B^2 \times 0.52$, where A is the longest diameter of tumor and B is the shortest diameter.[29]

H. Xenograft-Derived Cells

Tumors were minced into small pieces and then digested for 2 hours with collagenase type II in phosphate-buffered saline. Samples were then run through a cell filter (40 μM, Thermo Fisher Scientific) and plated into T-25 flasks. The medium was replaced after 72 hours and routine culture was carried out once cells reached confluence.

I. Statistics

A one way ANOVA with multiple comparisons was used to calculate *p*-values to determine the statistical significance of the difference in means. For tumor incidence, significance was determined by the chi-squared test. Statistical tests were considered significant at $p < 0.05$ and were performed using Prism 7 software (GraphPad Software, La Jolla, CA, USA).

III. RESULTS

A. Chromium-Transformed BEAS-2B Cells Do Not Exhibit Mitochondrial Respiratory Dysfunction

BEAS-2B cells chronically treated with 0.5 μM Cr(VI) [6 months (180 days)] generated colonies in soft agar (data not shown). We developed Cr(VI)-transformed cells (B2B-CrT) from an isolated colony collected from soft agar. Passaged-matched control BEAS-2B cells and B2B-CrT were analyzed for mitochondrial respiration using the Seahorse Analyzer and the mitochondrial stress test assay. The basal respiration, maximal respiration, and spare respiratory capacity of the Cr(VI)-transformed cells (B2B-CrT) were not different from passaged-matched control BEAS-2B cells (Fig. 1C). The proton leak, non-mitochondrial

oxygen consumption, and coupling efficiency were unchanged in the transformed cells compared with the passage-matched control cells (Fig. 1D,E). Interestingly, the transformed cells had a higher coupled respiration (Fig. 1D). These data indicated that Cr(VI)-transformed BEAS-2B cells did not display mitochondrial respiratory dysfunction and may be more metabolically active.

B. Chromium-Transformed BEP2D Cells Do Not Exhibit Mitochondrial Respiratory Dysfunction

Because cancer cells usually display some mitochondrial respiratory dysfunction, we tested whether our findings were cell specific by comparing with other Cr(VI)-transformed cell types. We received HPV (E6 and E8) immortalized bronchial epithelial airway cells (BEP2D cells) and Cr(VI)-transformed BEP2D cells (BPD-CrT) from Dr. John P. Wise, Sr.8 Passage-matched control BEP2D cells and BPD-CrT were analyzed for mitochondrial respiration using the Seahorse Analyzer and the mitochondrial stress test assay.

The basal respiration, maximal respiration, and spare respiratory capacity of the transformed cells were not different from passaged-matched control BEP2D cells (Fig. 2A–C). The proton leak and non-mitochondrial oxygen consumption were un-changed in the transformed cells compared with the passage-matched control cells (Fig. 2D). The coupled respiration and coupling efficiency were not statically different from passaged-matched control cells (Fig. 2D,E). These data indicated that BPD-CrT cells did not display mitochondrial respiratory dysfunction. These results are consistent with results from BEAS-2B cells.

C. Chromium-Transformed Lung Fibroblasts Do Not Exhibit Mitochondrial Respiratory Dysfunction

As mentioned before, we were surprised to find no major respiration changes in our Cr(VI)-transformed cells. To further show that our findings were not unique to immortalization factor or cell type, we compared our results with h-TERT immortalized fibroblasts. We obtained immortalized human lung fibroblast cells (WTHBF-6 cells) and Cr(VI)-transformed WTHBF-6 cells (T23-3 and T73-3) from Dr. John P. Wise, Sr.[22] These three different cell lines also allowed us to determine whwether immortalization or cell type plays a role. Passaged-matched control WTHBF-6 (C52-2), T23-3, and T73-3 cells were analyzed for mitochondrial respiration using the Seahorse Analyzer and the mitochondrial stress test assay. The basal respiration, maximal respiration, and spare respiratory capacity of the Cr(VI)-transformed fibroblasts were not different from passaged-matched control fibroblast cells (Fig. 3A–C). The proton leak, non-mitochondrial oxygen consumption, coupling efficiency, and coupled respiration were unchanged in the transformed cells compared with the passage-matched control cells (Fig. 3D,E). These data indicated that Cr(VI)-transformed fibroblasts did not display mitochondrial respiratory dysfunction and confirmed the results of the epithelial cell lines, suggesting that immortalization factors did not play any role.

D. Cr(VI)-Transformed Cells Grow Tumors in Nude Mice

It was important to further demonstrate that our Cr(VI)-transformed cells were malignantly transformed because we did not observe any changes in mitochondrial respiratory

dysfunction and most cancer cell lines and tumors reported in the literature exhibit mitochondrial dysfunction.[19] We used the xenograft tumor growth assay to demonstrate that all sets of Cr(VI)-transformed cells were malignantly transformed and were able to induce tumors in Nude mice. We injected all sets of the transformed cells and their passaged-matched control cells into Nude mice. Our results showed that B2B-CrT, BPD-CrT, T23-3, and T73-3 cells were able to grow tumors in Nude mice (Figs. 4–6). None of the passaged-matched control cells grew tumors in Nude mice. These data from the tumorigenesis experiments confirm that our Cr(VI)-transformed cells were malignantly transformed.

E. Cr(VI)-Lung Fibroblast Xenograft-Derived Cells Have Mitochondrial Respiratory Dysfunction

Carcinogenesis is considered a multi-step process. The mechanism of metal-induced carcinogenesis can be conceptualized into two stages. During the first stage, normal cells undergo neoplastic transformation into malignantly transformed cells. In this stage, Cr(VI)-induced cellular transformation did not induce mitochondrial respiratory dysfunction. The second stage is the progression from malignantly transformed cells into tumors (tumorigenesis).[30] We investigated whether xenograft tumor-derived cells have mitochondrial respiration changes. This would further provide evidence that the tumor microenvironments may drive some of the mitochondrial dysfunctions found in cancer cells reported in the literature. From the WTHBF-6 Cr(VI)-transformed cell lines' xenograft tumor tissues, we isolated cells. Specifically, we isolated six cell lines from the T23-3 xenograft tumor tissues and two cell lines from the T73-3 xenograft tumor tissues. Passaged-matched control WTHBF-6 cells (C52-2), two Cr(VI)-trans-formed colonies (T23-3 and T73-3), and the xenograft tumor-derived cell lines (T23-3-X2, T23-3-X3, T23-3-X4, T23-3-X5, T23-3-X6, T23-3-X7, T73-3-X2, and T73-3-X3) were analyzed for mitochondrial respiration. Again, mitochondrial respiration was measured using the Seahorse Analyzer.

The basal respiration of xenograft tumor-derived cells were not different between passaged-matched control cells (C52-2 cells) and Cr(VI)-transformed cells (T23-3 and T73-3 cells) (Fig. 7A,B,E,F). Xenograft tumor-derived cells showed decreases in maximal respiration and spare respiratory capacity compared with the passage-matched control cells and the transformed cell lines (except for T23-3-X3, which had increased respiration). The proton leak was higher in T23-3-X5, T23-3-X6, T23-3-X7, T73-3-X3, and T73-3-X3 cells compared with passaged-matched control cells (C52-2) (Fig. 7C,G). In most of the xenograft tumor-derived cell lines (T23-3-X2, T23-3-X4, T23-3-X5, T23-3-X6, T23-3-X7, T73-3-X2, and T73-3-X3), coupled respiration was higher than the passaged-matched control cells (Fig. 7C,G). Non-mitochondrial oxygen consumption was lower in all the xenograft tumor-derived cells except for T73-3-X2.All of the xenograft tumor-derived cells showed decreased mitochondrial coupling efficiency compared with passaged-matched control fibroblasts and Cr(VI)-transformed cells. These data demonstrate that xenograft tumor-derived cells showed mitochondrial respiratory dysfunction and provided evidence that mitochondrial dysfunction observed in cancer may be, at least in part, due to tumor microenvironments.

IV. DISCUSSION

Over the last few decades, significant progress has been made in our understanding of the mechanisms of Cr(VI)-induced carcinogenesis, including the roles of reactive oxygen species, genomic instability, and DNA damage repair deficiency in Cr(VI) carcinogenic mechanism.[6–8] However, some pathways believed to be important in cancer pathogenesis remain to be investigated (i.e., immortalization factors, growth signaling pathways, and energy metabolism). It has been established that altered energy metabolism is important for carcinogenesis and cancer cell survival. Specifically, increased lipid synthesis, the "Warburg effect," and mitochondrial dysfunction are known to be important metabolic changes in cancer cells.[16–18] There is limited literature on mitochondrial dysfunction during the transformation process of malignant cell transformation.

Previously, it was shown that human skin fibroblasts treated with a high concentration (5 μM) of Cr(VI) generated cell populations that were resistant to Cr(VI) toxicity and survived treatment. These cells exhibit no mitochondrial DNA damage compared with control passaged-matched cells. However, these cells had a decreased spare respiratory capacity compared with control.[31] It is important to note that, in our Cr(VI)-transformed cells, we did not see major changes in their spare respiratory capacity as observed with skin fibroblasts in the aforementioned study. There are two possible explanations for this: (1) the previous studies focused on acute, high-Cr(VI) exposures and this change could be related to survival during acute Cr(VI) exposure, and (2) another report found that human lung and skin fibroblasts have different sensitivities to Cr(VI).[32]

In the present study, we report on mitochondrial respiration in multiple sets of Cr(VI)-transformed lung cells compared with their passage-matched control cells. We also report on the mitochondrial respiration of xenograft tumor-derived cells. Previously, it was shown that Cr(VI) cancer stem-like cells had decreased oxygen consumption compared with passaged-matched control BEAS-2B cells and BEAS-2B Cr-(VI)-transformed cells.[33] It has been established in other studies that cancer stem cells have different metabolism compared with cancer cells, which would explain the difference in results obtained from Cr(VI) cancer stem-like cells and our current study.[33,34] Another study reported that acute exposure to Cr(VI) could cause mitochondrial dysfunction.[10] It is important to note that this difference from our results could be due to toxicity of Cr(VI) at 48 hours and may represent a survival response to acute Cr(VI) toxicity and that the changes reported are not necessarily part of the Cr(VI)-induced carcinogenic mechanism.

Through measuring functional mitochondrial respiration, our results indicate that mitochondrial respiration is not affected negatively in Cr(VI)-transformed lung cells compared with passaged-matched control cells. We observe that most of Cr(VI)-transformed cells have increased coupled respiration, but some Cr(VI)-transformed cells do not. The xenograft tumor-derived cells have increased coupled respiration compared with their Cr(VI)-transformed cell counter. The observed differences in some of the respiration functions between the transformed cells could be due to the fact that some mitochondrial changes in the cells are not uniform during cellular transformation and other metabolic end

points (e.g., glycolysis, lipid synthesis, mitochondrial membrane potential, and mitochondrial DNA changes) could also be involved.

We report on the mitochondrial respiration of cells derived from xenograft tumor tissues. We found that xenograft tumor-derived cells had significant inhibition of their maximum mitochondrial respiration and spare respiratory capacity. These cells also had decreased coupling efficiency, which is another end point showing mitochondrial respiratory dysfunction. Conversely, one cell line (T23-3-X2) showed increased mitochondrial respiration, suggesting that not every cell from a tumor undergoes mitochondrial dysfunction. These data indicate that cellular transformation does not drive mitochondrial dysfunction; rather, it may be due to the tumor microenvironment.

Treatment of immortalized prostate epithelial cells with ethidium bromide causes depletion of mitochondrial DNA, which has been a critical factor in various cancer end points (e.g., survival, migration, and glycolytic metabolism).[35] Patient-derived pancreatic cancer cell lines had mutations in their mitochondrial DNA and further examination of the metabolic profiling led to the finding that complex I, III, and IV were inhibited in some of the patient-derived pancreatic cell lines.[16] In the same study, the investigators reported that, in the patient-derived pancreatic cell lines (with complex I inhibition), oxygen consumption was lower than that in immortalized pancreatic cells.[16] These patient-derived xenografts cell line results are in agreement with our results obtained from xenograft tumor-derived cells. In another report, human lung cells (BE-AS-2B) chronically (6 month) exposed to arsenic were reported to have mitochondrial dysfunction. The investigators measured the end point of gene expression and found that multiple genes associated with mitochondrial dysfunction were lower in the arsenic-treated cells compared with the passaged-matched control BEAS-2B cells. Specifically, the expressions of genes associated with the electron transport chain were lower.[21]

Although there was no mitochondrial respiratory dysfunction in Cr(VI)-transformed cells, it is possible that other end points of mitochondrial dysfunction may be present. These include mitochondrial DNA damage, mitophagy dysfunction, and changes to the mitochondrial membrane potential. Because respiration is unaffected in these cells, it is likely that the mitochondrial membrane potential is unaffected. Future studies are needed to investigate the cause of mitochondrial respiration changes in xenograft tumor-derived cells. Specifically, the role of Nrf2 in the mitochondrial changes needs to be investigated given that Nrf2 is upstream of some metabolism pathways and this transcription factor is constitutively activated in Cr(VI)-transformed cells compared with passaged-matched control cells.[1–3,29,36] Further, when constitutively activated, Nrf2 plays an oncogenic role in cancer development. It is also likely that Nrf2 may not properly regulate metabolism end points as described previously in the literature and may be a major cause for metabolism shifts.[36] The changes in the mitochondrial membrane potential, mitochondrial DNA, and mitophagy during Cr(VI)-transformation and in xenograft tumor-derived cells remain to be determined.

In conclusion, the results from the present study show that, during the early stage of metal-induced carcinogenesis [normal cells to malignantly transformed human lung cells due to exposure to Cr(VI)] does not result in mitochondrial respiratory dysfunction. These results

were not cell-type specific (fibroblast vs. epithelial cells). In the second stage of metal-induced carcinogenesis (transformed cells to tumor), we observed mitochondrial respiratory dysfunction. Therefore, our results obtained from xenograft-tumor derived cells suggest that mitochondrial respiratory dysfunction occurs during the later stage of Cr(VI)-induced carcinogenesis (transformed cells to tumor).

ACKNOWLEDGMENTS

The authors thank Hong Lin from the University of Kentucky for technical and administrative support.

We thank Dr. John P. Wise, Sr., University of Louisville (Louisville, KY), for the use of the WTHBF-6 Cells, and Dr. Curtis Harris, National Institute of Health, for the use of the BEP2D cells.

This work was supported by NIH (Grants R01ES021771, R01ES020870, R01ES025515, R01ES28984, R01ES21771, and P30ES026529) and the Redox Metabolism Shared Resource Facility of the University of Kentucky Markey Cancer Center (Grant P30CA177558).

REFERENCES

1. Kim D, Dai J, Fai LY, Yao H, Son YO, Wang L, Pratheeshkumar P, Kondo K, Shi X, Zhang Z. Constitutive activation of epidermal growth factor receptor promotes tumorigenesis of Cr(VI)-transformed cells through decreased reactive oxygen species and apoptosis resistance development. J Biol Chem 2015;290(4):2213–24. [PubMed: 25477514]
2. Kim D, Dai J, Park YH, Yenwong Fai L, Wang L, Pratheeshkumar P, Son YO, Kondo K, Xu M, Luo J, Shi X, Zhang Z. Activation of epidermal growth factor receptor/p38/hypoxia-inducible factor-1α is pivotal for angiogenesis and tumorigenesis of malignantly transformed cells induced by hexavalent chromium. J Biol Chem 2016;291(31):16271–81. [PubMed: 27226640]
3. Son YO, Pratheeshkumar P, Wang L, Wang X, Fan J, Kim DH, Lee JY, Zhang Z, Lee JC, Shi X. Reactive oxygen species mediate Cr(VI)-induced carcinogenesis through PI3K/AKT-dependent activation of GSK-3β/β-catenin signaling. Toxicol Appl Pharmacol 2013; 271(2):239–48. [PubMed: 23707771]
4. Tsuneta Y, Ohsaki Y, Kiyonobu K, Mikami H, Abe S, Murao M. Chromium content of lungs of chromate workers with lung cancer. Thorax 1980;35(4):294–7. [PubMed: 7434272]
5. Wang L, Wise JTF, Zhang Z, Shi X. Progress and prospects of free radicals in metal-induced carcinogenesis. Curr Pharmacol Rep 2016; 2(4):178–86. [PubMed: 27617186]
6. Wang X, Son YO, Chang Q, Sun L, Hitron JA, Budhraja A, Zhang Z, Ke Z, Chen F, Luo J, Shi X. NADPH oxidase activation is required in reactive oxygen species generation and cell transformation induced by hexavalent chromium. Toxicol Sci 2011;123(2):399–410. [PubMed: 21742780]
7. Wise SS, Holmes AL, Wise JP, Sr. Hexavalent chromium-induced DNA damage and repair mechanisms. Rev Environ Health 2008;23(1):39–57. [PubMed: 18557597]
8. Xie H, Holmes AL, Wise SS, Huang S, Peng C, Wise JP, Sr. Neoplastic transformation of human bronchial cells by lead chromate particles. Am J Respir Cell Mol Biol 2007;37(5):544–52. [PubMed: 17585109]
9. Abreu PL, Ferreira LMR, Alpoim MC. Impact of hexavalent chromium on mammalian cell bioenergetics: phenotypic changes, molecular basis and potential relevance to chromate-induced lung cancer. Biometals 2014;27(3):409–43. [PubMed: 24664226]
10. Cerveira JF, Sánchez-Aragó M, Urbano AM, Cuezva JM. Short-term exposure of nontumorigenic human bronchial epithelial cells to carcinogenic chromium(VI) compromises their respiratory capacity and alters their bioenergetic signature. FEBS Open Bio 2014;26;4:594–601.
11. Guo L, Xiao Y, Wang Y. Hexavalent chromium-induced alteration of proteomic landscape in human skin fibroblast cells. J Proteome Res 2013;12(7):3511–8. [PubMed: 23718831]
12. Clementino M, Shi X, Zhang Z. Oxidative stress and metabolic reprogramming in Cr(VI) carcinogenesis. Curr Opin Toxicol 2018;8:20–7. [PubMed: 29568811]

13. Warburg O, Wind F, Negelein E. The metabolism of tumors in the body. J Gen Physiol 1927;8(6): 519–30. [PubMed: 19872213]
14. Warburg O On the origin of cancer cells. Science 1956;123(3191):309–14. [PubMed: 13298683]
15. Warburg O On respiratory impairment in cancer cells. Science 1956;124(3215):269–70. [PubMed: 13351639]
16. Hanahan D, Weinberg RA. Hallmarks of cancer: the next generation. Cell 2011;144(5):646–74. [PubMed: 21376230]
17. Otto AM. Warburg effect(s): A biographical sketch of Otto Warburg and his impacts on tumor metabolism. Cancer Metab 2016;4:5. [PubMed: 26962452]
18. Santos CR, Schulze A. Lipid metabolism in cancer. FEBS J 2012;279(15):2610–23. [PubMed: 22621751]
19. Hsu CC, Tseng LM, Lee HC. Role of mitochondrial dysfunction in cancer progression. Exp Biol Med (May-wood) 2016;241(12):1281–95.
20. Hardie RA, van Dam E, Cowley M, Han TL, Balaban S, Pajic M, Pinese M, Iconomou M, Shearer RF, McKenna J, Miller D, Waddell N, Pearson JV, Grimmond SM; Australian Pancreatic Cancer Genome Initiative, Sazanov L, Biankin AV, Villas-Boas S, Hoy AJ, Turner N, Saunders DN Mitochondrial mutations and metabolic adaptation in pancreatic cancer. Cancer Metab 2017;5:2. [PubMed: 28163917]
21. Stueckle TA, Lu Y, Davis ME, Wang L, Jiang BH, Holaskova I, Schafer R, Barnett JB, Rojanasakul Y. Chronic occupational exposure to arsenic induces carcinogenic gene signaling networks and neoplastic transformation in human lung epithelial cells. Toxicol Appl Pharmacol 2012;261(2):204–16. [PubMed: 22521957]
22. Wise SS, Aboueissa AE, Martino J, Wise JP, Sr. Hexavalent chromium-induced chromosome instability drives permanent and heritable numerical and structural changes and a dna repair-deficient phenotype. Cancer Res 2018;78(15):4203–14. [PubMed: 29880483]
23. Ke Y, Reddel RR, Gerwin BI, Miyashita M, McMenamin M, Lechner JF, Harris CC. Human bronchial epithelial cells with integrated SV40 virus T antigen genes retain the ability to undergo squamous differentiation. Differentiation 1988;38(1):60–6. [PubMed: 2846394]
24. Willey JC, Broussoud A, Sleemi A, Bennett WP, Cerutti P, Harris CC. Immortalization of normal human bronchial epithelial cells by human papillomaviruses 16 or 18. Cancer Res 1991;51(19): 5370–7. [PubMed: 1717149]
25. Wise SS, Elmore LW, Holt SE, Little JE, Antonucci PG, Bryant BH, Wise JP, Sr. Telomerase-mediated lifespan extension of human bronchial cells does not affect hexavalent chromium-induced cytotoxicity or genotoxicity. Mol Cell Biochem 2004;255(1–2):103–11. [PubMed: 14971651]
26. Wise JP, Sr, Wise SS, Little JE. The cytotoxicity and genotoxicity of particulate and soluble hexavalent chromium in human lung cells. Mutat Res 2002;517(1–2):221–9. [PubMed: 12034323]
27. Mitov MI, Harris JW, Alstott MC, Zaytseva YY, Evers BM, Butterfield DA. Temperature induces significant changes in both glycolytic reserve and mitochondrial spare respiratory capacity in colorectal cancer cell lines. Exp Cell Res 2017;354(2):112–21. [PubMed: 28342898]
28. Chang Q, Pan J, Wang X, Zhang Z, Chen F, Shi X. Reduced reactive oxygen species-generating capacity contributes to the enhanced cell growth of arsenic-transformed epithelial cells. Cancer Res 2010;70(12):5127–35. [PubMed: 20516118]
29. Pratheeshkumar P, Son YO, Divya SP, Turcios L, Roy RV, Hitron JA, Wang L, Kim D, Dai J, Asha P, Zhang Z, Shi X. Hexavalent chromium induces malignant transformation of human lung bronchial epithelial cells via ROS-dependent activation of miR-21-PDCD4 signaling. Oncotarget 2016;7(32):51193–210. [PubMed: 27323401]
30. Xu J, Wise JTF, Wang L, Schumman K, Zhang Z, Shi X. Dual roles of oxidative stress in metal carcinogenesis. J Environ Pathol Toxicol Oncol 2017;36(4):345–76. [PubMed: 29431065]
31. Nickens KP, Han Y, Shandilya H, Larrimore A, Gerard GF, Kaldjian E, Patierno SR, Ceryak S. Acquisition of mitochondrial dysregulation and resistance to mitochondrial-mediated apoptosis after genotoxic insult in normal human fibroblasts: a possible model for early stage carcinogenesis. Biochim Biophys Acta 2012;1823(2): 264–72. [PubMed: 22057391]

32. Xie H, Holmes AL, Wise SS, Young JL, Wise JTF, Wise JP Sr. Human skin cells are more sensitive than human lung cells to the cytotoxic and cell cycle arresting impacts of particulate and soluble hexavalent chromium. Biol Trace Elem Res 2015;166(1):49–56. [PubMed: 25805272]

33. Dai J, Ji Y, Wang W, Kim D, Fai LY, Wang L, Luo J, Zhang Z. Loss of fructose-1,6-bisphosphatase induces glycolysis and promotes apoptosis resistance of cancer stem-like cells: an important role in hexavalent chromium-induced carcinogenesis. Toxicol Appl Pharmacol 2017;331:164–73. [PubMed: 28624442]

34. Dong BW, Qin GM, Luo Y, Mao JS. Metabolic enzymes: key modulators of functionality in cancer stem-like cells. Oncotarget 2017;8(8):14251–67. [PubMed: 28009990]

35. Moro L, Arbini AA, Yao JL, di Sant'Agnese PA, Marra E, Greco M. Mitochondrial DNA depletion in prostate epithelial cells promotes anoikis resistance and invasion through activation of PI3K/Akt2. Cell Death Differ 2009;16(4):571–83. [PubMed: 19079138]

36. Wang YY, Chen J, Liu XM, Zhao R, Zhe H. Nrf2-mediated metabolic reprogramming in cancer. Oxid Med Cell Longev 2018;2018:9304091. [PubMed: 29670683]

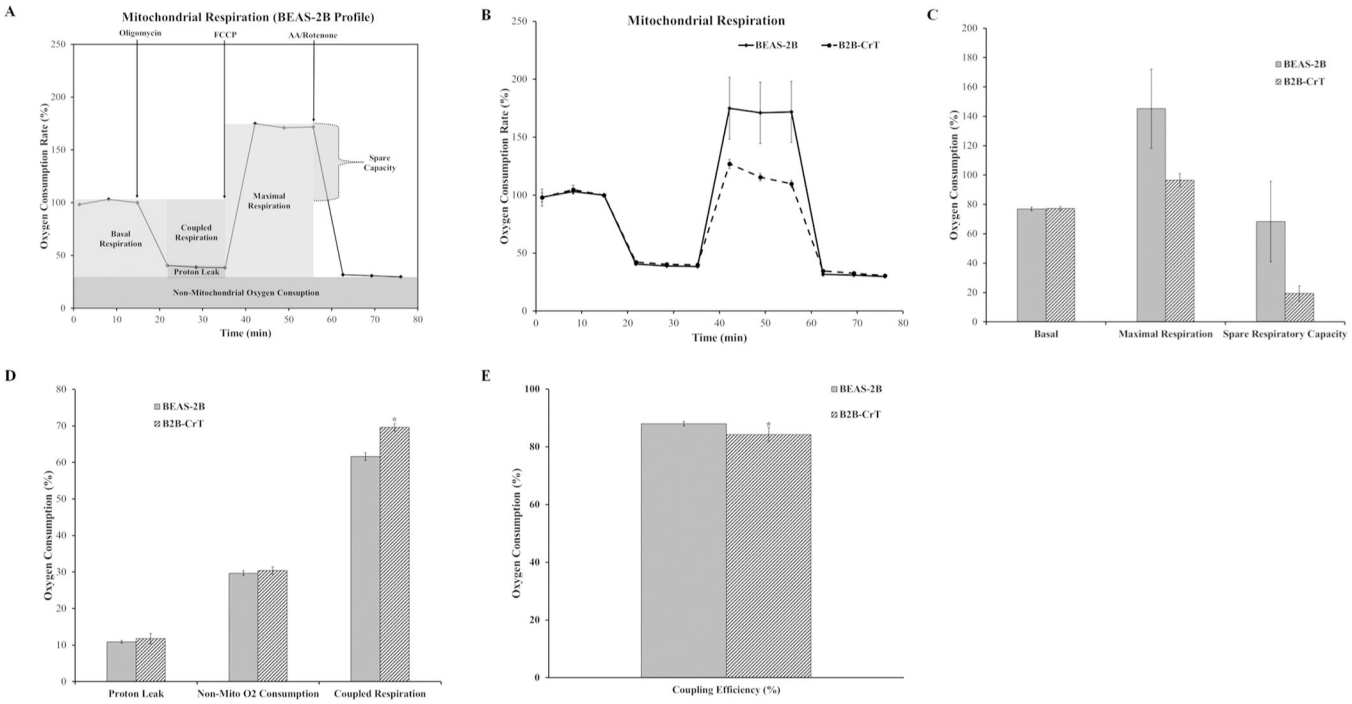

FIG. 1:

C(VI)-transformed bronchial airway epithelial cells (BEAS-2B) do not have mitochondrial respiratory dysfunction. (A) Mitochondrial respiration profile for BEAS-2B cells with the relevant injection strategy for the Seahorse Analyzer mitochondrial stress test. (B) Oxygen consumption data for BEAS-2B and B2B-CrT cells presented as a baseline percentage to the third oxygen consumption read. (C) Basal respiration, maximal respiration, and spare respiratory capacity for the BEAS-2B and B2B-CrT cells. (D) Proton leak, non-mitochondrial oxygen consumption, and coupled respiration for BEAS-2B and B2B-CrT cells. (E) Mitochondrial coupling efficiency for BEAS-2B and B2B-CrT cells. Data are the average of at least three experiments ± SEM. $*p < 0.05$.

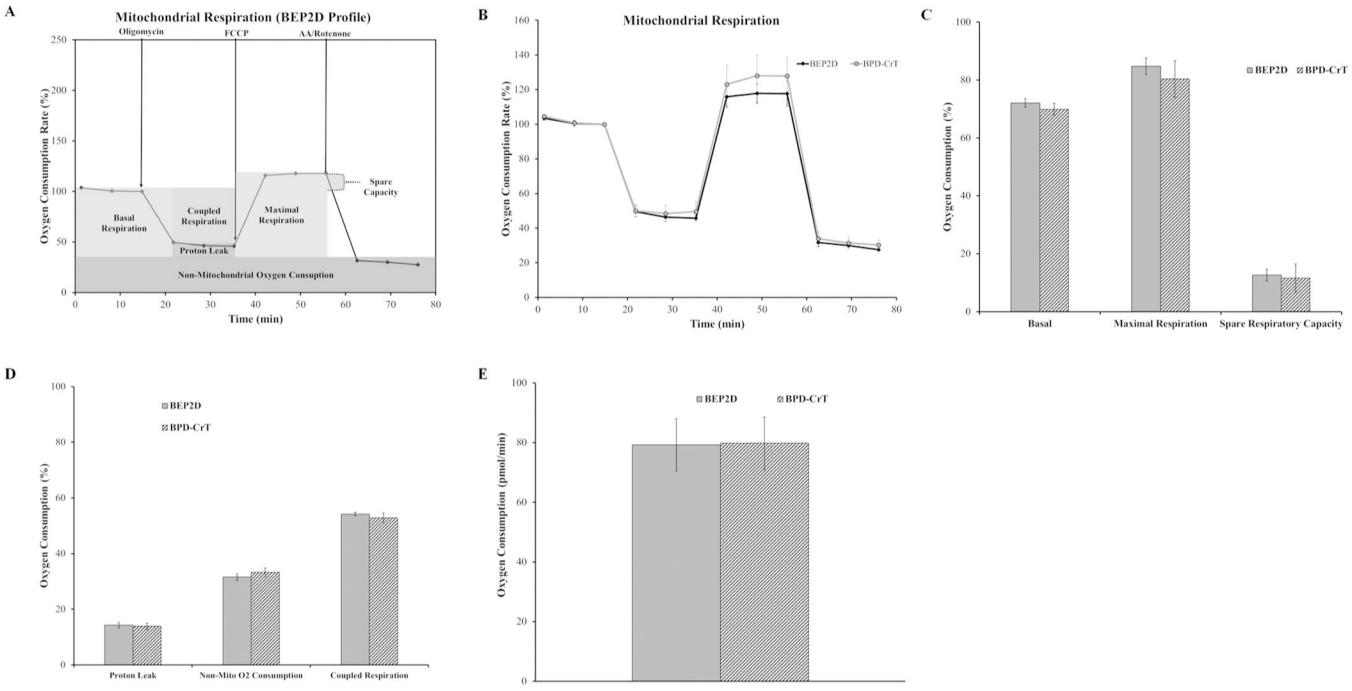

FIG. 2:

C(VI)-transformed bronchial airway epithelial cells (BEP2D) do not have mitochondrial respiratory dysfunction. (A) Mitochondrial respiration profile for BEP2D cells with the relevant injection strategy for the Seahorse Analyzer mitochondrial stress test. (B) Oxygen consumption data for BEP2D and BPD-CrT cells presented as a baseline percentage to the third oxygen consumption read. (C) Basal respiration, maximal respiration, and spare respiratory capacity for BEP2D and BPD-CrT cells. (D) Proton leak, non-mitochondrial oxygen consumption, and coupled respiration for BEP2D and BPD-CrT cells. (E) Mitochondrial coupling efficiency for BEP2D and BPD-CrT cells. Data for B–E are the average of at least three experiments ± SEM. $*p < 0.05$.

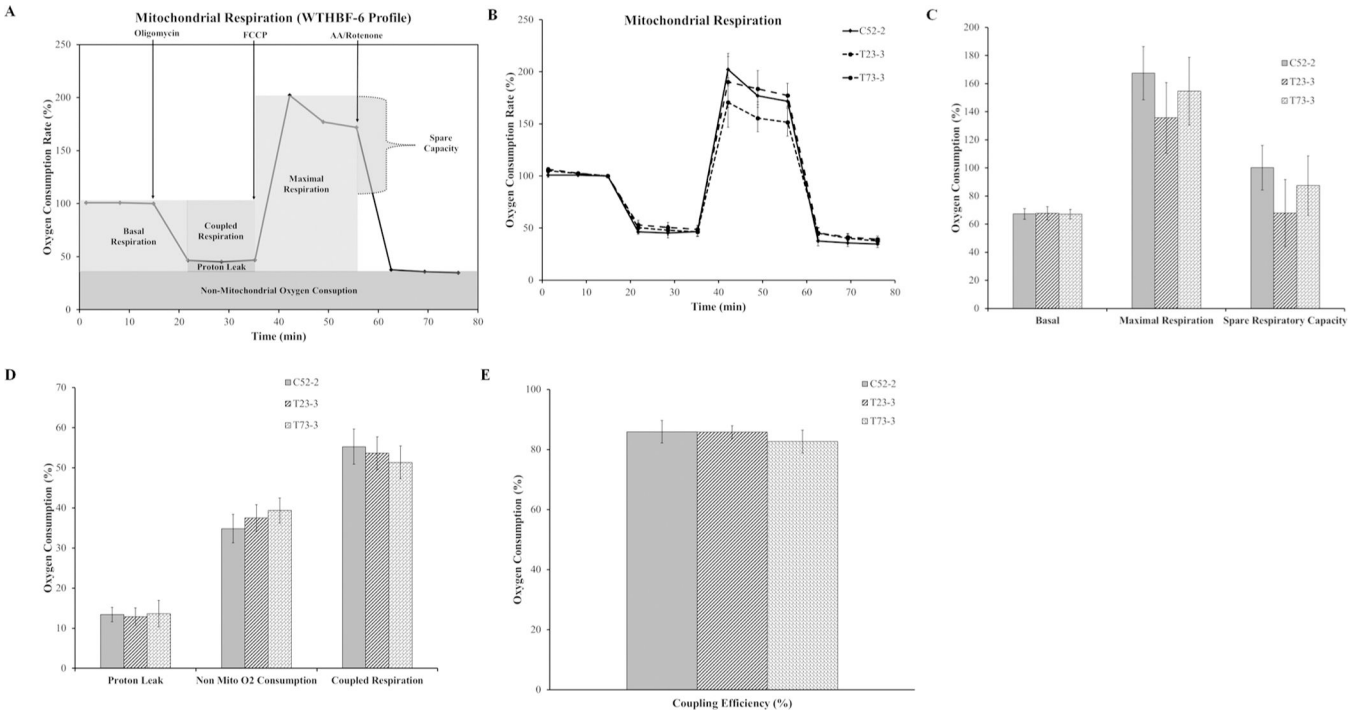

FIG. 3:

C(VI)-transformed human lung fibroblasts (WTHBF-6) do not have mitochondrial respiratory dysfunction. (A) Mitochondrial respiration profile for WTHBF-6 cells with the relevant injection strategy for the Seahorse Analyzer mitochondrial stress test. (B) Oxygen consumption data for the control WTHBF-6 cells (C52-2 cells) and Cr(VI)-transformed WTHBF-6 cells (T23-3 and T73-3 cells) presented as a baseline percentage to the third oxygen consumption read. (C) Basal respiration, maximal respiration, and spare respiratory capacity for C52-2, T23-3, and T73-3 cells. (D) Proton leak, non-mitochondrial oxygen consumption, and coupled respiration for C52-2, T23-3, and T73-3 cells. (E) Mitochondrial coupling efficiency for C52-2, T23-3, and T73-3 cells. Data are the average of at least three experiments ± SEM. $*p < 0.05$.

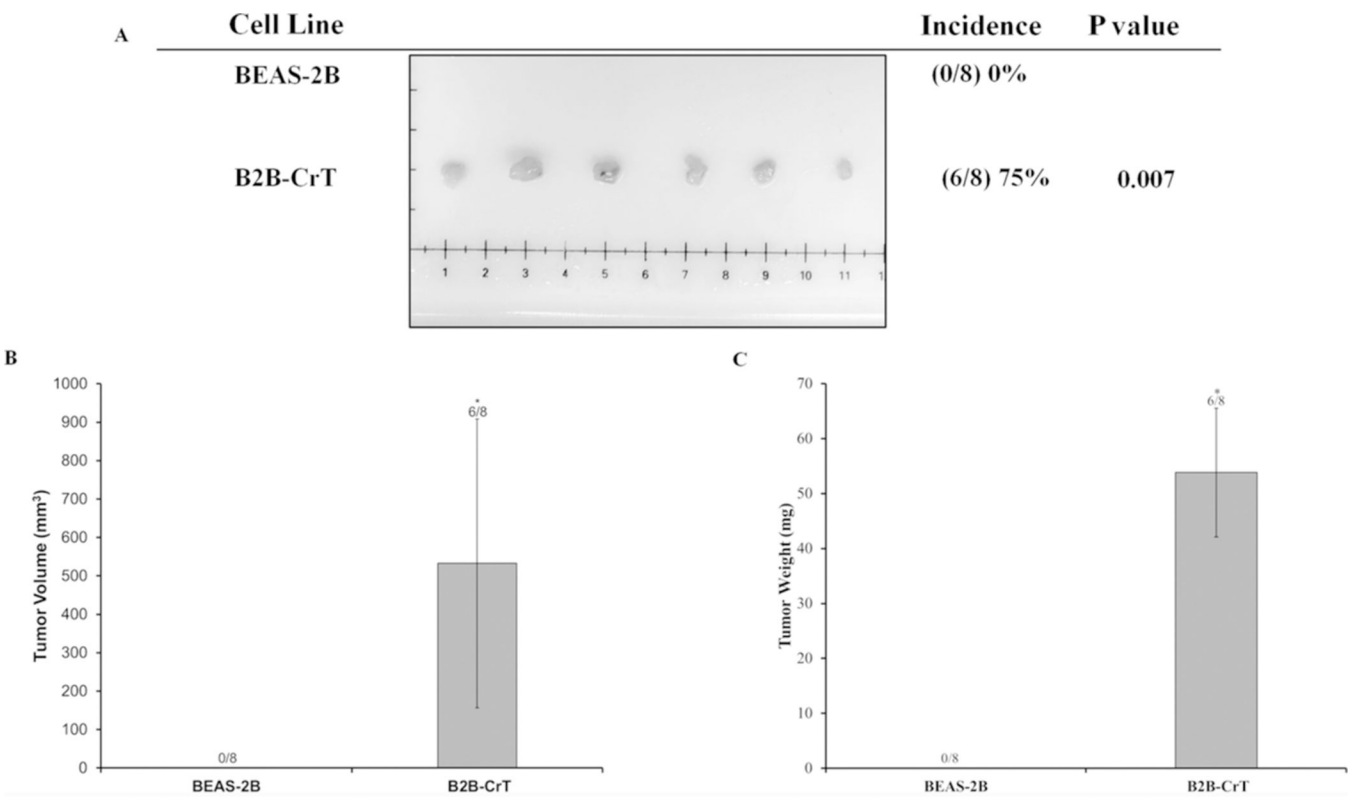

FIG. 4:

C(VI)-transformed human lung bronchial cells (BEAS-2B cells) grow tumors in Nude mice. Passage-matched control BEAS-2B cells and Cr(VI)-transformed BEAS-2B cells (B2B-CrT cells) were injected into the flanks of 6-week-old athymic Nude mice (1×10^6 cells per mouse) and checked weekly for tumor appearance. There were eight subcutaneous injection sites per cell line. (A) Tumor incidences. (B) Tumor volume measured after euthanasia. Tumor volume was determined by calipers following the formula $A \times B^2 \times 0.52$, where A is the longest diameter of tumor and B is the shortest diameter. (C) Tumor weights. Data are expressed as the mean ± SEM.

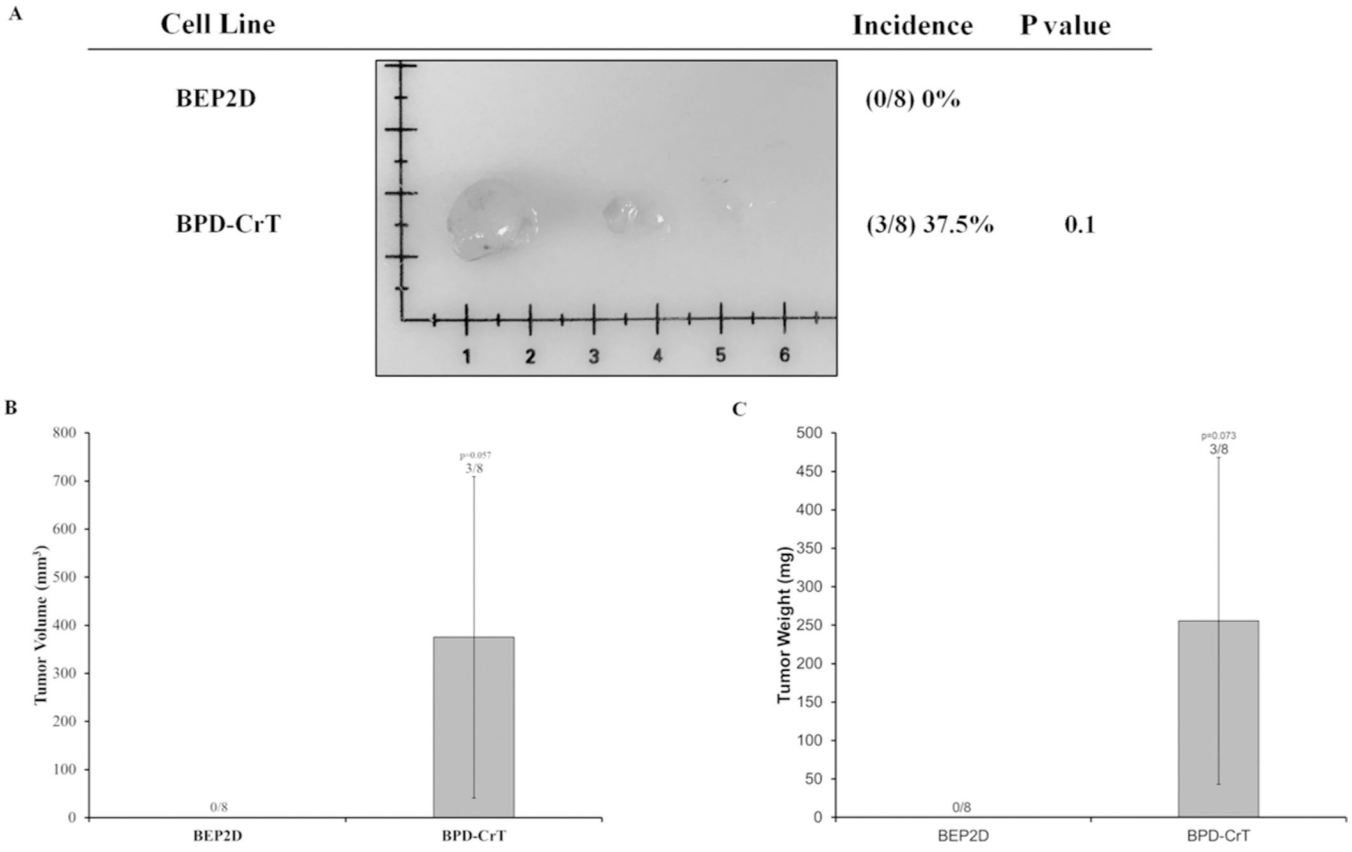

FIG. 5:

C(VI)-transformed human lung bronchial cells (BEP2D cells) grow tumors in Nude mice. Passage-matched control BEP2D cells and Cr(VI)-transformed BEP2D cells (BPD-CrT cells) were injected subcutaneously into the flanks of 6-week-old athymic Nude mice (1×10^6 cells per mouse) and checked weekly for tumor appearance. There were eight subcutaneous injection sites per cell line. (A) Tumor incidences. (B) Tumor volume measured after euthanasia. Tumor volume was determined by calipers following the formula $A \times B^2 \times 0.52$, where A is the longest diameter of tumor and B is the shortest diameter. (C) Tumor weights. Data are expressed as the mean ± SEM.

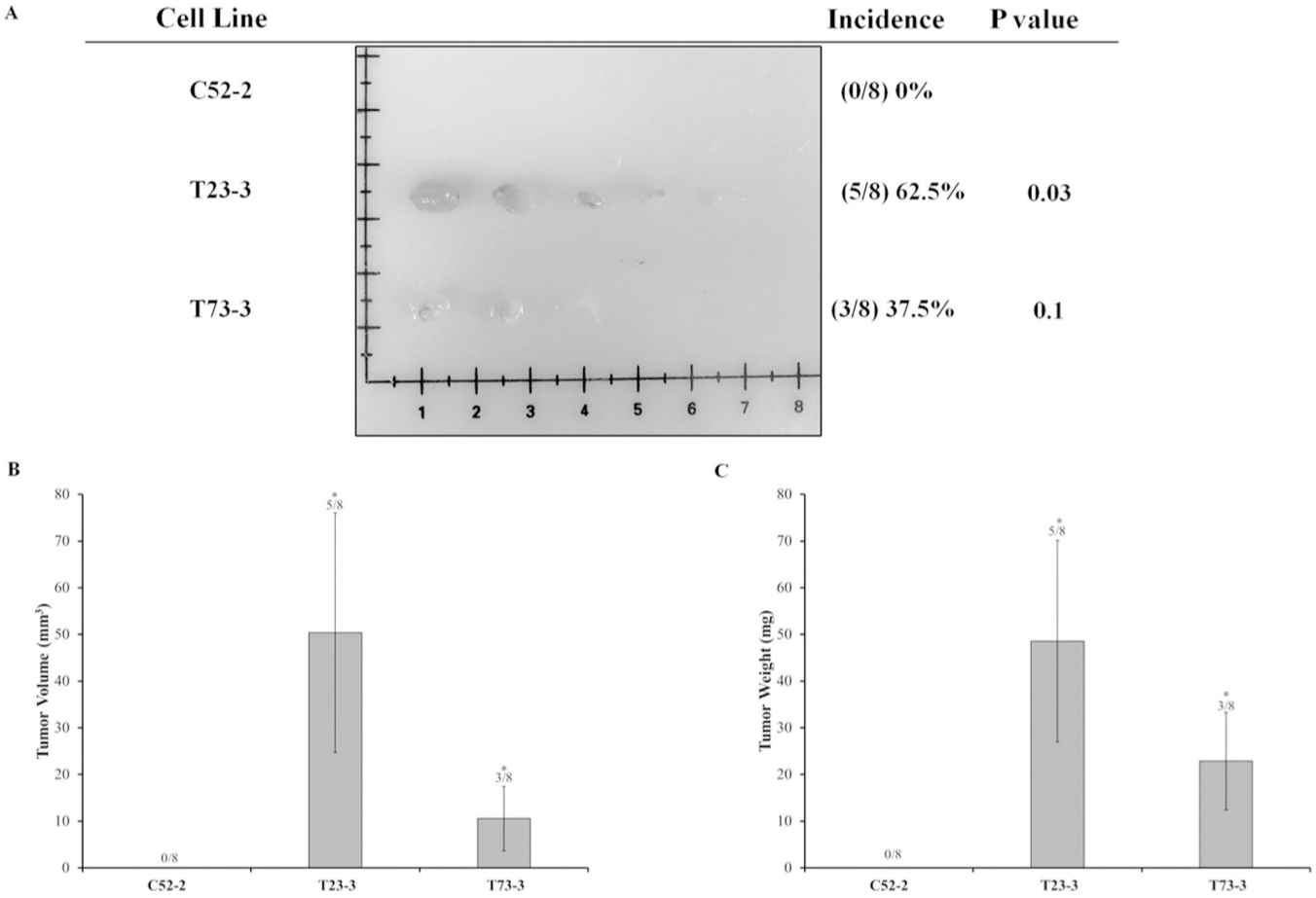

FIG. 6:

C(VI)-transformed human lung fibroblasts (WTHBF-6 cells) grow tumors in Nude mice. Passage-matched control WTHBF-6 cells (C52-2 cells) and Cr(VI)-transformed WTHBF-6 cells (T23-3 and T73-3 cells) were injected subcutaneously into the flanks of 6-week-old athymic Nude mice (1×10^6 cells per mouse) and checked weekly for tumor appearance. There were eight subcutaneous injection sites per cell line. (A) Tumor incidences. (B) Tumor volume measured after euthanasia. Tumor volume was determined by calipers following the formula $A \times B^2 \times 0.52$, where A is the longest diameter of tumor and B is the shortest diameter. (C) Tumor weights. Data are expressed as the mean ± SEM.

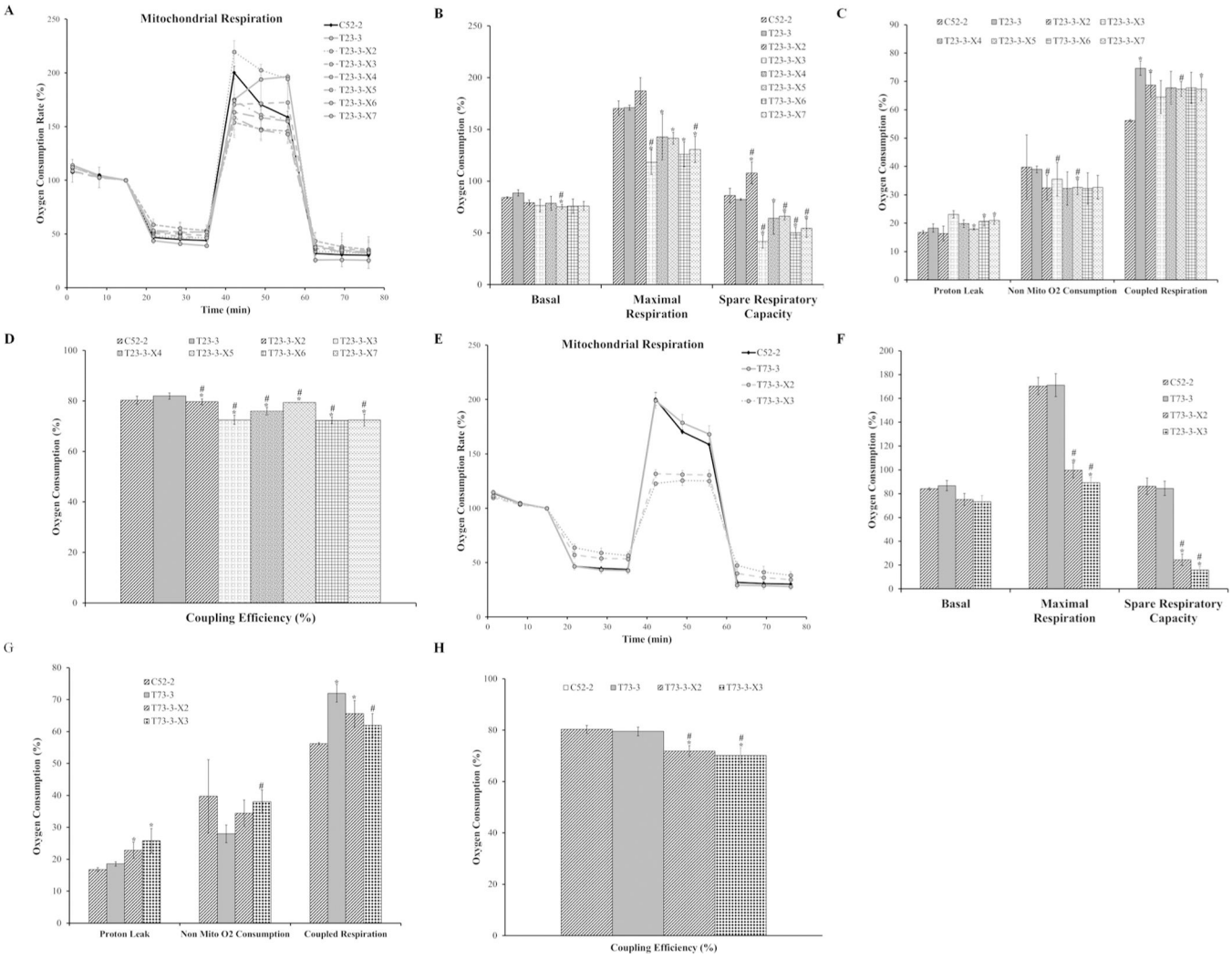

FIG. 7:

Xenograft tumor-derived cells have dysfunctional mitochondrial respiration. (A) Oxygen consumption data for the control WTHBF-6 cells (C52-2 cells) and Cr(VI)-transformed WTHBF-6 cells (T23-3 cells) and xenograft tumor-derived cells (T23-3-X2, T23-3-X3, T23-3-X4, T23-3-X5, T23-3-X6, and T23-3-X7 cells) presented as a baseline percentage to the third oxygen consumption read. (B) Basal respiration, maximal respiration, and spare respiratory capacity for C52-2, T23-3, T23-3-X2, T23-3-X3, T23-3-X4, T23-3-X5, T23-3-X6, and T23-3-X7 cells. (C) Proton leak, non-mitochondrial oxygen consumption, and coupled respiration for C52-2, T23-3, T23-3-X2, T23-3-X3, T23-3-X4, T23-3-X5, T23-3-X6, and T23-3-X7 cells. (D) Mitochondrial coupling efficiency for C52-2, T23-3, T23-3-X2, T23-3-X3, T23-3-X4, T23-3-X5, T23-3-X6, and T23-3-X7 cells. (E) Oxygen consumption data for control WTHBF-6 cells (C52-2 cells), Cr(VI)-transformed WTHBF-6 cells (T73-3 cells), and xenograft tumor-derived cells (T73-3-X2 and T73-3-X3 cells) presented as a baseline percentage to the third oxygen consumption read. (F) Basal respiration, maximal respiration, and spare respiratory capacity for the C52-2, T73-3, T73-3-X2, and T73-3-X3 cells. (G) Proton leak, non-mitochondrial oxygen consumption, and coupled respiration for

C52-2, T73-3, T73-3-X2, and T73-3-X3 cells. (H) Mitochondrial coupling efficiency for C52-2, T73-3, T73-3-X2, and T73-3-X3 cells. Data are the average of at least three experiments ± SEM. *$p < 0.05$ from C52-2 cells. #$p < 0.05$ from either T23-3 or T73-3 cells.